

Supporting Information

Hollow CuSe nanocubes as bifunctional electrocatalyst for energy-saving overall urea-water electrolysis

Shouyi Wang^{#, a}, Siyu Liu^{#, a}, Ying Yang^{*, a}, Jiayao Jiang^a, Leijiao Li^{*, a}, Tingting Wang^{*, a, b}

^a Key Laboratory of Applied Chemistry and Nanotechnology at Universities of Jilin Province, Changchun University of Science and Technology, Changchun 130022, China.

^b Chongqing Research Institute, Changchun University of Science and Technology, No.5 Yulin Road, Longxing Town, Yubei District, Chongqing City 401135, China.

Email: yangying0807@126.com; lileijiao@cust.edu.cn; Wangtt@cust.edu.cn

[#] These authors contributed equally to this work.

Experimental Section

Chemicals

Copper sulfate pentahydrate ($\text{CuSO}_4 \cdot 5\text{H}_2\text{O}$) and sodium hydroxide were purchased from Sinopod Group Chemical Reagent Co., LTD. Polyvinylpyrrolidone (PVP), selenium dioxide (SeO_2), ascorbic acid, DL-tartaric acid, D (+) glucose, selenium powder, sodium citrate, copper citrate were purchased from Shanghai Aladdin Biochemical Technology Co., LTD. Urea ($\text{CH}_4\text{N}_2\text{O}$) was from Tianjin Zhiyuan chemical reagent Co., Ltd. Potassium hydroxide (KOH) was purchased from Jindong Tianzheng Fine Chemical Reagent Factory. Pt/C (20 wt.%, Pt on Vulcan XC-72R) and Nafion (5 wt%) were obtained from Aldrich. All reagents are analytically pure and used directly without further purification and all aqueous solutions were prepared with ultrapure water ($18.2 \text{ M}\Omega \cdot \text{cm}$) obtained from a Millipore system.

Physical Characterizations

The morphology and microstructure were observed by transmission electron microscope (TEM Tecnai G2 F20). The Crystalline phase of the synthesized sample was tested by Y-2000 X-ray diffractometer (XRD) with the 2θ ranges from 10° to 80° at a scanning rate of $10^\circ \text{ min}^{-1}$.

Electrochemical Measurements

Electrochemical HER performance was tested on an electrochemical workstation (CHI 660e) in 1 M KOH solution at room temperature, using a standard three-electrode system. The synthesized catalyst was selected as the working electrode, Hg/HgO electrode as the reference electrode, and carbon rod as the counter electrode. The

polarization curves were recorded by linear sweep voltammetry (LSV) technique at $5 \text{ mV}\cdot\text{s}^{-1}$ with iR correction. In addition, the current density is calculated on the basis of the actual electrode area ($0.5 \times 0.5 \text{ cm}^2$) immersed in the electrolyte. All of the measured potentials were showed versus reversible hydrogen electrode (RHE) following the equation: $E_{\text{RHE}}=E_{\text{Hg/HgO}} + 0.098 \text{ V}+0.059 \text{ pH}$. According to the reported electrochemical method, the electrochemical active surface area (ECSA) of the catalyst modified electrode was calculated by double-layer capacitor (C_{dl}). The cyclic voltammograms (CVs) were tested with different rates from 20 to $100 \text{ mV}\cdot\text{s}^{-1}$. Electrochemical impedance spectroscopy (EIS) was performed at a current density of $10 \text{ mA}\cdot\text{cm}^{-2}$. All impedance data have been fitted. For long-term stability tests, which were carried out at $10 \text{ mV}\cdot\text{s}^{-1}$. The long-term durability test of CuSe/NF electrode was tested by constant current electrolysis.

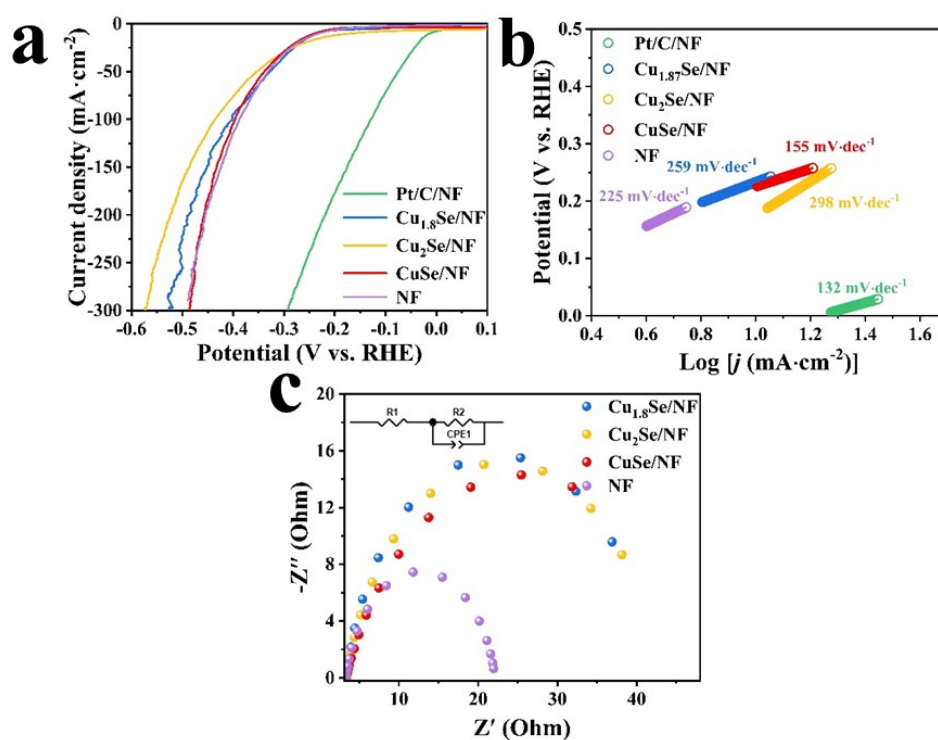


Fig. S1 (a) LSV curves towards the HER of Pt/C/NF, Cu_{1.8}Se/NF, Cu₂Se /NF, CuSe/NF and NF in 1.0 M KOH; (b) Tafel slopes towards the HER in 1.0 M KOH; (c) EIS curves at $10 \text{ mA}\cdot\text{cm}^{-2}$ towards the HER in 1.0 M KOH.

Table S1 Comparison of HER properties of CuSe/NF with other catalysts.

Catalyst	j (mA cm ⁻²)	η (mV)	Ref.
CuSe/NF	10	199	This work
Zn-MoSe ₂	10	182	1
Cu ₂ Se@NiFe-LDHNS	10	205	2
Cu ₃ P/Cu ₂ Se	10	166	3
Cu-Ni ₃ S ₂ /NF	10	188	4
NiCo-WSe ₂	10	205	5

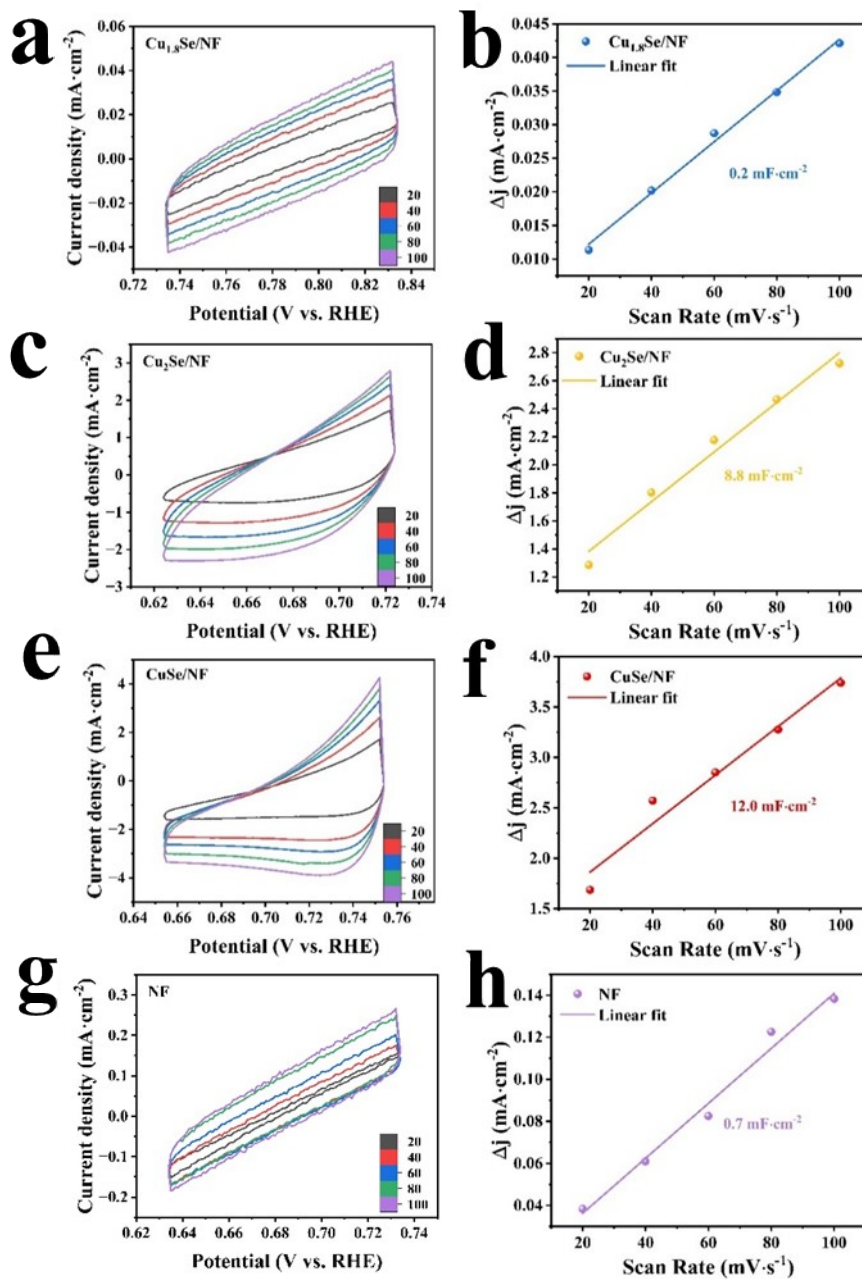


Fig. S2 Cyclic voltammograms at scan rates from 20-100 $\text{mV}\cdot\text{s}^{-1}$. Samples measured in a non-Faradaic region at different scan rates in 1 M KOH + 0.5 M urea electrolyte: (a, b) $\text{Cu}_{1.8}\text{Se}/\text{NF}$, (c, d) $\text{Cu}_2\text{Se}/\text{NF}$, (e, f) CuSe/NF and (g, h) NF .

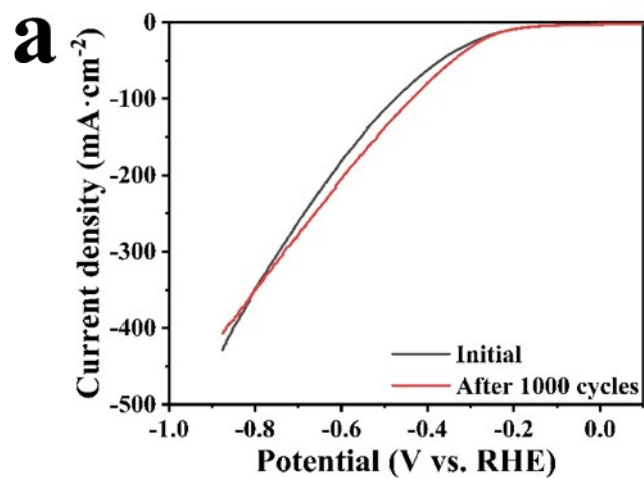


Fig. S3 (a) Polarization curves of CuSe/NF for the HER before and after 1000 CV cycles in 1 M KOH + 0.5 M urea.

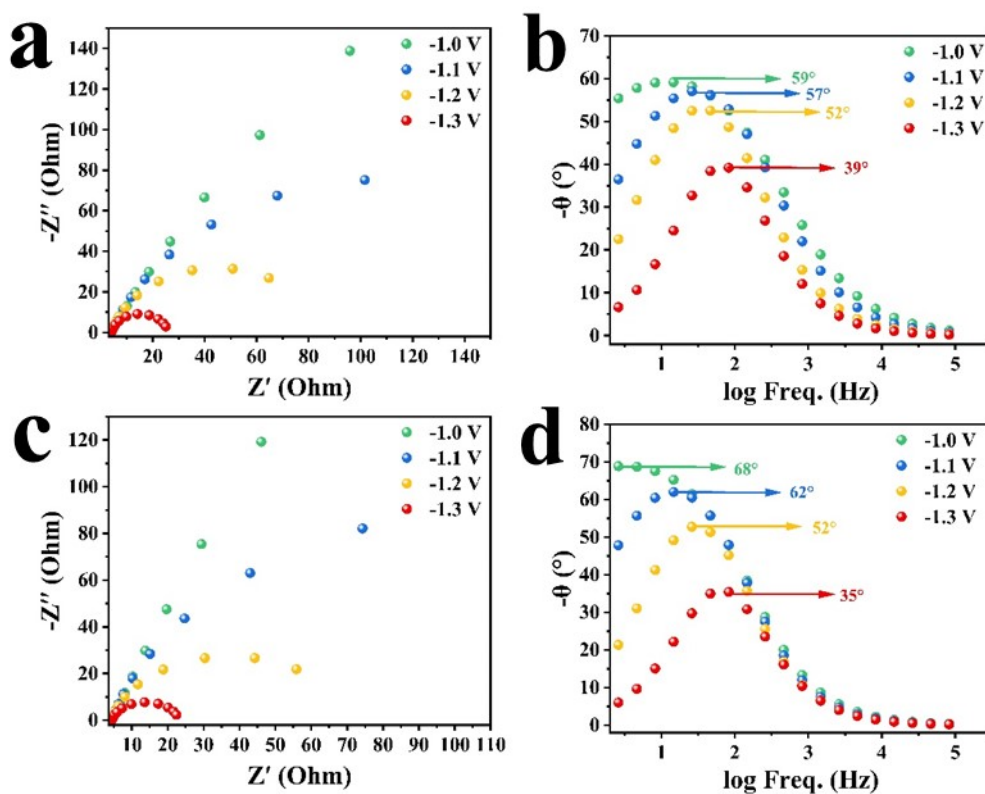


Fig. S4 Nyquist and Bode plots at different potentials (-1.0, -1.1, -1.2, and -1.3 V vs. SCE) for (a, b) $\text{Cu}_{1.8}\text{Se}/\text{NF}$ and (c, d) $\text{Cu}_2\text{Se}/\text{NF}$ in 1 M KOH + 0.5 M urea electrolyte.

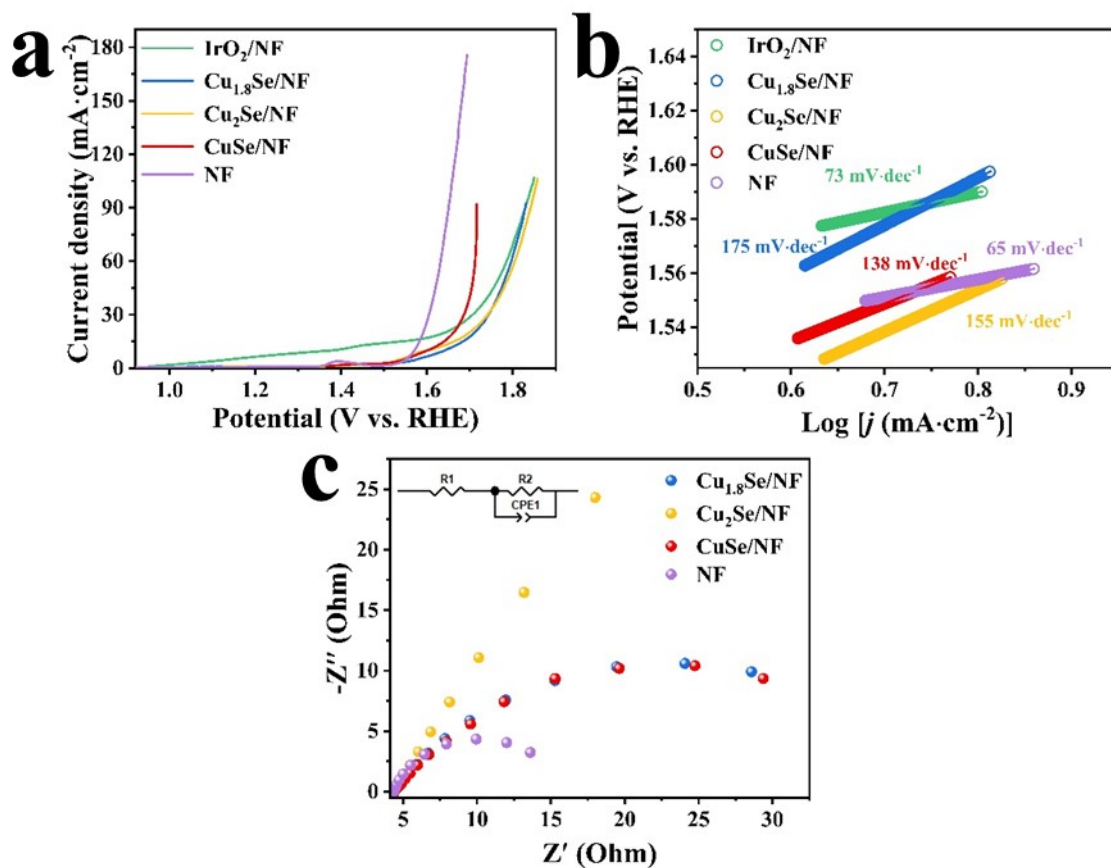


Fig. S5 (a) LSV curves towards the OER of Pt/C/NF, Cu_{1.8}Se/NF, Cu₂Se /NF, CuSe/NF and NF in 1.0 M KOH; (b) Tafel slopes towards the OER in 1.0 M KOH; (c) EIS results at 10 mA·cm⁻² towards the OER in 1.0 M KOH.

Table S2 Comparison of UOR properties of CuSe/NF with other catalysts.

Catalyst	j (mA cm ⁻²)	η (V)	Ref.
CuSe/NF	10	1.38	This work
NiCo ₂ S ₄ @Ni ₃ Se ₂	10	1.396	6
Cu ₃ P@CuO _x	10	1.37	7
Se-CoS ₂ NW/CF	10	1.46	8
NiMoSe	10	1.39	9
Cu ₃ P-NW/CF	10	1.43	10

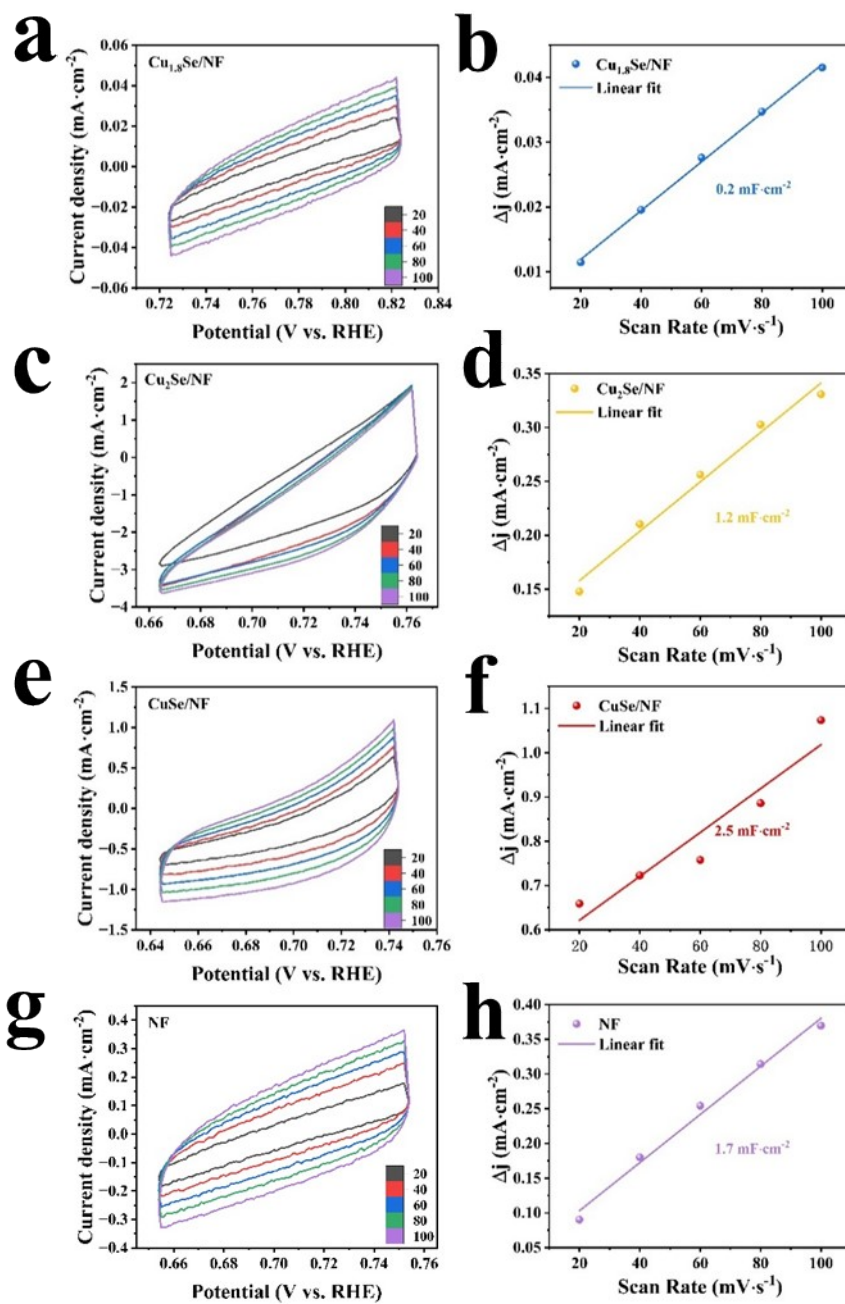


Fig. S6 Cyclic voltammograms at scan rates from 20-100 $\text{mV}\cdot\text{s}^{-1}$. Samples measured in a non-Faradaic region at different scan rates in 1 M KOH + 0.5 M urea electrolyte: (a, b) $\text{Cu}_{1.8}\text{Se}/\text{NF}$, (c, d), $\text{Cu}_2\text{Se}/\text{NF}$ (e, f), CuSe/NF and (g, h) NF .

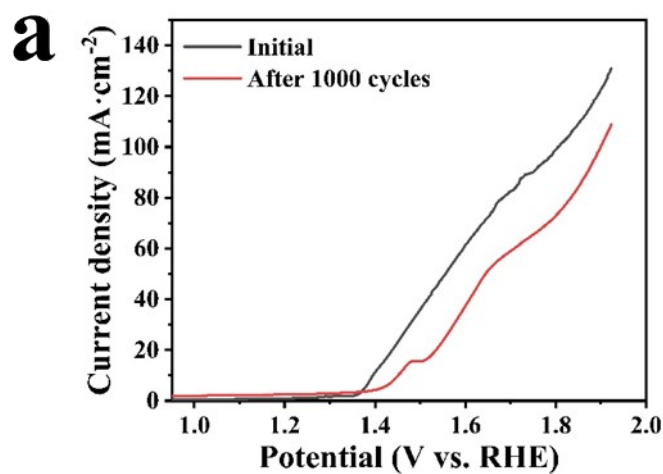


Fig. S7. (a) Polarization curves of CuSe/NF for the UOR before and after 1000 CV cycles.

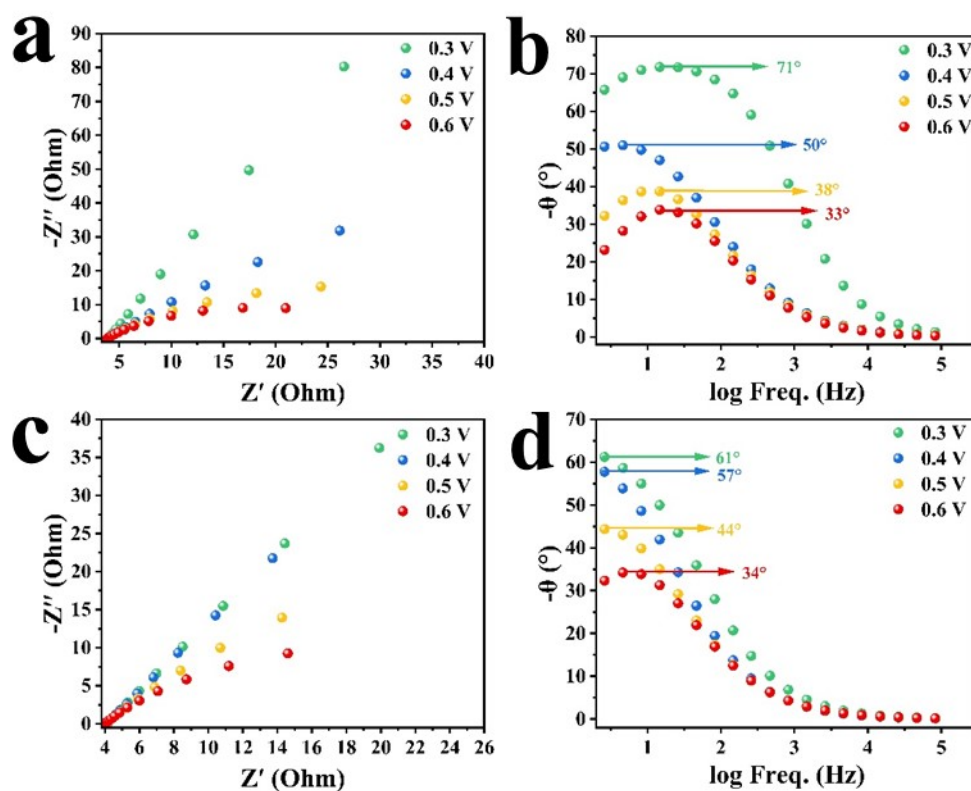


Fig. S8 Nyquist and Bode plots at different potentials (0.3, 0.4, 0.5, and 0.6V vs. SCE) for (a, b) $\text{Cu}_{1.8}\text{Se}/\text{NF}$ and (c, d) $\text{Cu}_2\text{Se}/\text{NF}$ in 1 M KOH + 0.5 M urea electrolyte.

Reference

1. J. Qian, T. Wang, B. Xia, P. Xi and D. Gao, *Electrochimica Acta*, 2019, **296**, 701-708.

2. H. Qi, P. Zhang, H. Wang, Y. Cui, X. Liu, X. She, Y. Wen and T. Zhan, *J Colloid Interface Sci*, 2021, **599**, 370-380.
3. C. An, Y. Wang, R. Huang, Y. Li, C. Wang, S. Wu, L. Gao, C. Zhu, Q. Deng and N. Hu, *Colloids and Surfaces A: Physicochemical and Engineering Aspects*, 2023, **667**, 131360.
4. M. Wei, D. Zhang, J. Deng, X. Xiao, L. Wang, X. Wang, M. Song, S. Wang, X. Zheng and X. Liu, *Industrial & Engineering Chemistry Research*, 2022.
5. F.-b. Guo, X.-y. Zhao, H.-y. Lei, Y. Xu, K.-k. Liu, L.-x. Zhang, J.-m. Xue and H.-r. Sun, *Journal of Alloys and Compounds*, 2022, **924**, 166538.
6. K. Cui, J. Fan, Z. Wang, G. Xiao, S. Gao, T. Huang, Z. Tan, C. Niu, W. Luo and Z. Chao, *Journal of Electroanalytical Chemistry*, 2023, **944**, 117681.
7. H. A. Bandal and H. Kim, *Applied Surface Science*, 2023, **622**, 156925.
8. Y. Tan, Y. Yin, X. Yin, C. Lan, Y. Wang, F. Hu, Q. Huang and Y. Mi, *Catalysts*, 2021, **11**, 169.
9. H. Wang, X. Jiao, W. Zeng, Y. Zhang and Y. Jiao, *International Journal of Hydrogen Energy*, 2021, **46**, 37792-37801.
10. H. Shen, T. Wei, J. Ding and X. Liu, *Materials (Basel)*, 2023, **16**, 4169.